香港科技大學
THE HONG KONG UNIVERSITY OF SCIENCE AND TECHNOLOGY

Aerodynamics Acoustics & Noise Control Technology Centre

A comparison of acoustic far-field prediction methods for turbulent flows

Siyang Zhong, Xin Zhang

The Hong Kong University of Science and Technology, Hong Kong, China

Sep. 21st , 2018, Svetlogorsk, Kaliningrad region, Russia.

Aerodynamics
Acoustics &
Noise Control
Technology
Centre

中航工业先进飞行器噪声技术中心
AVIC Advanced Aircraft Noise Technology Center

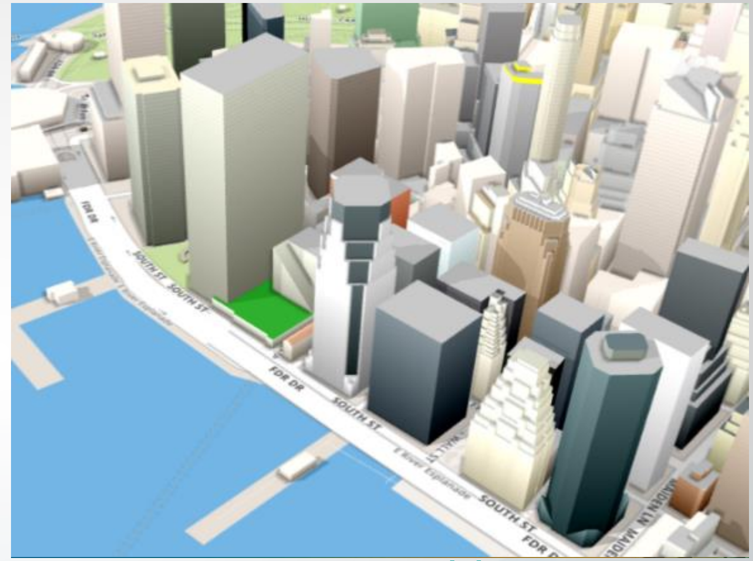

AANTC.ust.hk

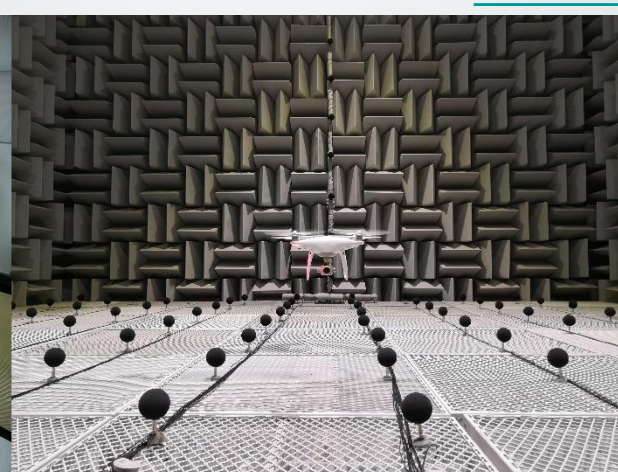

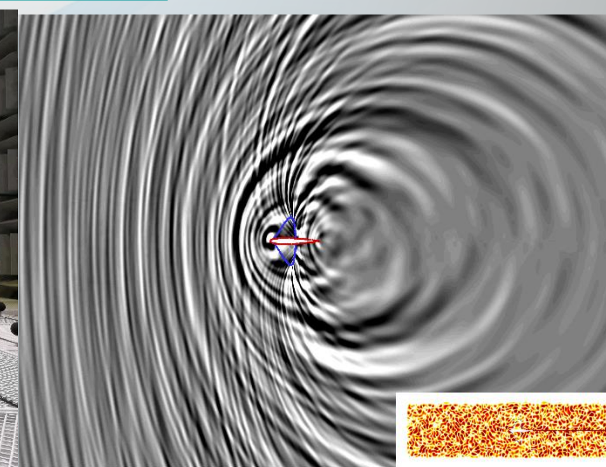

Contents

- Background.
- Acoustic far-field prediction methods based on surface integral solutions.
- Applications to a co-flowing jet.
- Summary.

Directivity in presence of turbulence

- Acoustic far-field directivity:
  - Integral solution of FW-H equation is widely used (Farassat, 1983).
  - The volume integral is often neglected for computational efficiency.
  - Spurious waves will be induced when there are convecting turbulence in an inhomogeneous background flow.

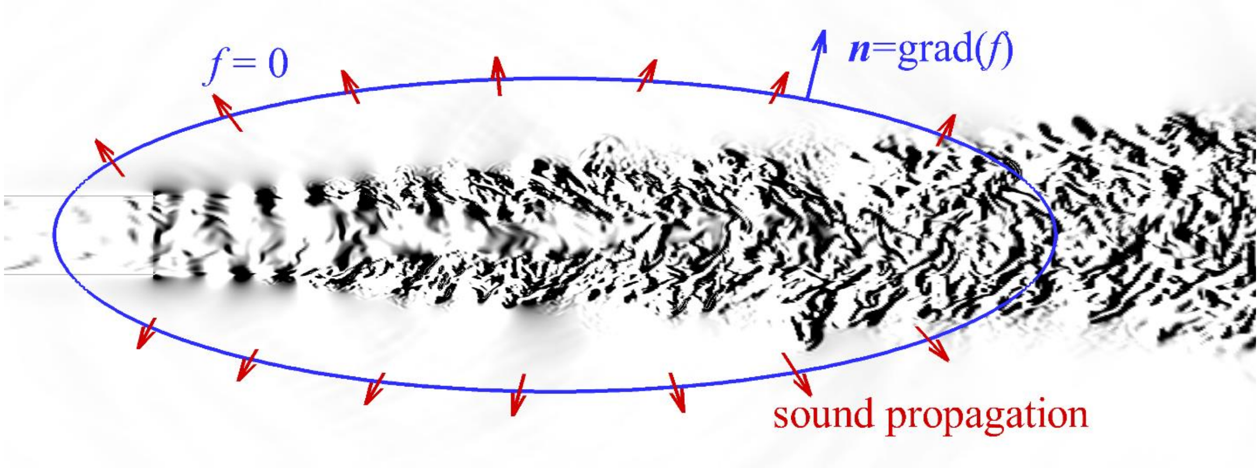

- There is a need to develop surface integral methods for robust, accurate computation of the far-field directivities to account for the presence of turbulence and non-uniform background mean flow.

Acoustic far-field prediction methods based on surface integral solutions

Existing strategies and methods

- Using on-body integration surfaces.

- Using open section integration surfaces.

- Using correction terms as substantial of the omitted volume sources (Lockard & Casper 2004; Ikeda *et al*. 2013, 2017; Rahier *et al*., 2015).

- Taking average of FW-H results by multiple integration surfaces (Shur *et al*. 2005; Spalart *et al*. 2009, 2011).

- Using a transition zone instead of single surface (Wright & Morfey, 2015).

These methods are mainly based on the FW-H equation.

Integral solutions to the FW-H equation

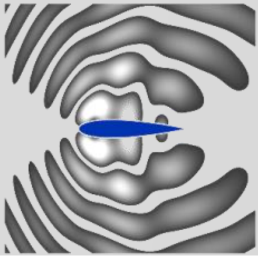

- The FW-H equation:

$$\left(\frac{\partial^2}{\partial t^2} - c_\infty^2 \frac{\partial^2}{\partial x_i \partial x_i}\right) p' = \frac{\partial^2}{\partial x_i \partial x_j}\left[T_{ij} H(f)\right]$$

$$+ \frac{\partial}{\partial t}\{[(\rho_\infty - \rho) v_n + \rho u_n]\delta(f)\} - \frac{\partial}{\partial x_i}\{\left[P_{ij} n_j + \rho u_i (u_n - v_n)\right]\delta(f)\}$$

- **M1**: Surface integral solution to the FW-H equation using a single integration surface (Brentner & Farassat, 1998).

- **M2**: Taking average of the results by different integration surfaces by **M1** (Shur *et al*. 2005; Spalart *et al*. 2009, 2011).

$$\hat{p}'(\boldsymbol{x}, \omega) = \frac{1}{N} \sum_{i=1}^{N} \hat{p}_i'(\boldsymbol{x}, \omega)$$

M0: use the indirect acoustic variable $\mathcal{D}_c p'$

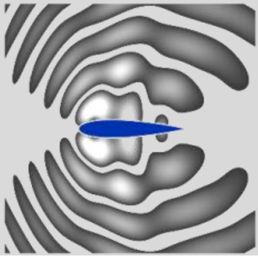

- In the near field of turbulent flow, the non-acoustic parts are also included in the flow variables.

- The principle idea is to filter out the non-acoustic components using some operators…

- The flow governing Eqs. are analogous to:

Sound propagation in the far-field

$$\left(\frac{\partial}{\partial t} + \boldsymbol{u}_\infty \cdot \nabla\right)\boldsymbol{u}' + \frac{\nabla p'}{\rho_\infty} = \boldsymbol{S}_u,$$

$$\left(\frac{\partial}{\partial t} + \boldsymbol{u}_\infty \cdot \nabla\right)p' + \gamma p_\infty \nabla \cdot \boldsymbol{u}' = S_p.$$

Remaining terms in the flow equation

- The eddies are mainly convected by the mean flow (Taylor, 1938):

$$\mathcal{D}_c(\cdot)' = \left(\frac{\partial}{\partial t} + \boldsymbol{u}_c \cdot \nabla\right)(\cdot)' \approx \left(\frac{\partial}{\partial t} + \boldsymbol{u}_c \cdot \nabla\right)(\cdot)'_a.$$

M0 : use the indirect acoustic variable $\mathcal{D}_c p'$

- Applying the operator $\mathcal{D}_c$ to the fluctuation variables and eliminate the variable $\mathcal{D}_c \boldsymbol{u}'$, we obtain that:

$$\mathcal{D}_\infty^2(\mathcal{D}_c p') - a_\infty^2 \nabla^2(\mathcal{D}_c p') = T_v.$$

- For sound extrapolation equations:

$$[\mathcal{D}_\infty^2 - c_\infty^2 \nabla^2][\mathcal{D}_c p' H(f)] = H(f) Q_v + \delta(f) Q_m + \frac{\partial}{\partial t}\left[Q_q \delta(f)\right] + \nabla \cdot [\boldsymbol{Q}\delta(f)].$$

- $\mathcal{D}_c p'$ is solved using the conventional Green's function
- p' is computed from $\mathcal{D}_c p'$ using the far-field approximation

$$\mathcal{D}_c p' = \frac{\partial p'_a}{\partial t} + u_\infty^i \frac{\partial p'_a}{\partial x_i} \to p'_a$$

Fourier transform

$\approx -\left(\frac{\Lambda_2^i}{a_\infty}\frac{\partial}{\partial t} + \frac{\Lambda_1^i}{X}\right) p'_a$, for $|\boldsymbol{x}| \gg |\boldsymbol{y}|$

M0: Definitions of p_0, $\boldsymbol{u_0}$ and $\boldsymbol{u_c}$

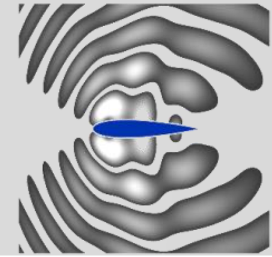

- There might be different definitions of the mean flow and fluctuation variables:
  - They should be identical to the mean flow variables in the far field.
  - Different definition can influence the source distributions of T_v.
- Definition of the mean pressure:

$$p_0 = \langle p \rangle = \lim_{T\to\infty} \frac{1}{T} \int_0^T p(t)\mathrm{d}t\,, \qquad p' = p - p_0.$$

- Definition of mean and convection velocity:

$$\boldsymbol{u}_0 = \boldsymbol{u_c} = \frac{\langle \rho \boldsymbol{u} \rangle}{\langle \rho \rangle}, \qquad \boldsymbol{u}' = \boldsymbol{u} - \boldsymbol{u}_0.$$

Applications to a co-flowing jet

Co-flowing jet noise

- $M_\infty = 0.2$, $M_j = 0.8$ and $R_e = 8000$, the flow is turbulent.
- An established DNS database (Sandberg & Tester, 2016).
- Off-body integration surfaces cross the jet region.

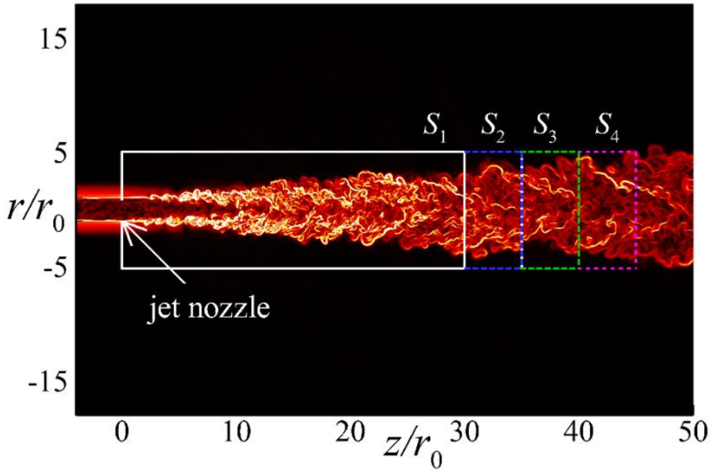

$|\nabla\rho|$

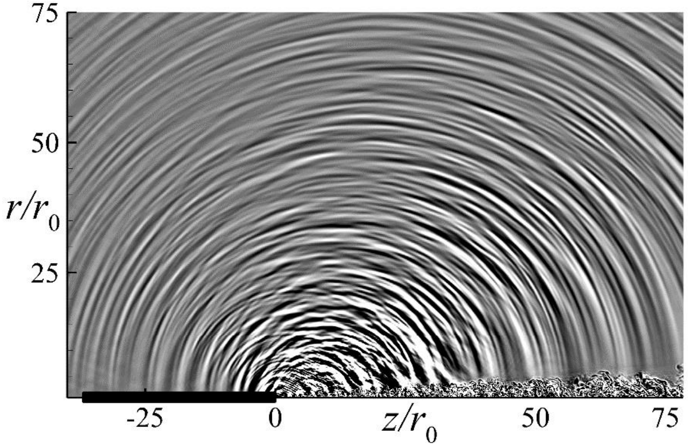

$\nabla \cdot \boldsymbol{u}$

Configurations

✈ Integration surfaces:

– Cylindrical permeable integration surface;

– The surface is closed in the jet region;

– The radius of the surfaces: $r = 4r_0$;

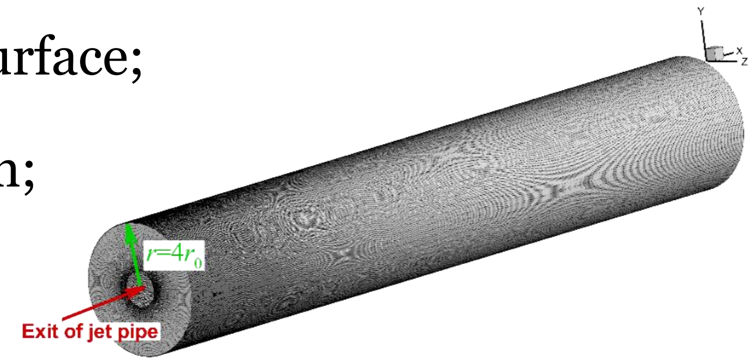

– Locations of of the surface ends:

Surfaces	**S1**	**S2**	**S3**	**S4**
Locations	$30r_0$	$35r_0$	$40r_0$	$45r_0$

– The source panels are assigned on the computational grid points;

– Observer distance is $r_o = 1000r_0$: sufficiently large.

M0: the predicted spectra

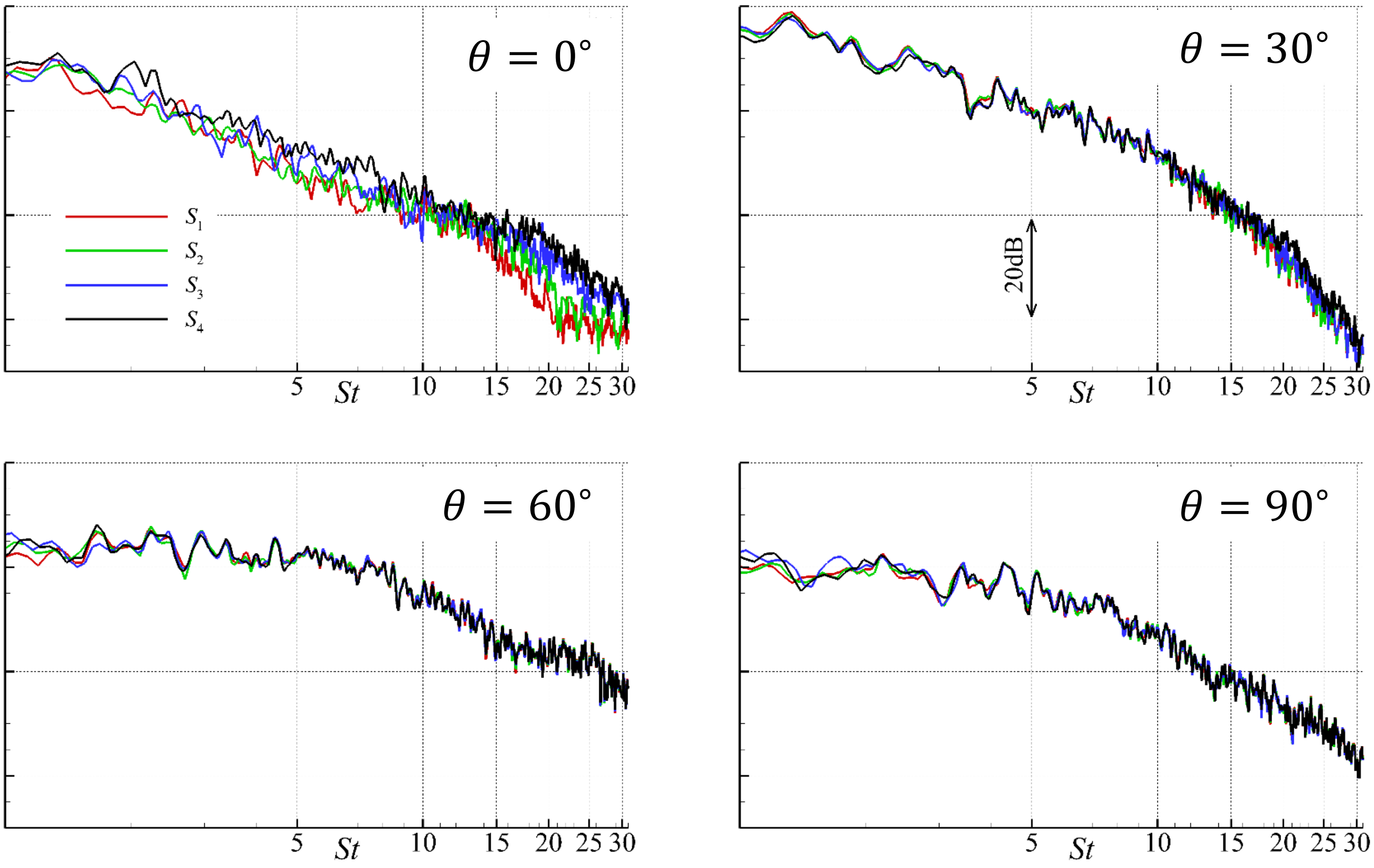

Zhong & Zhang, 2018

M0: the predicted far-field directivities

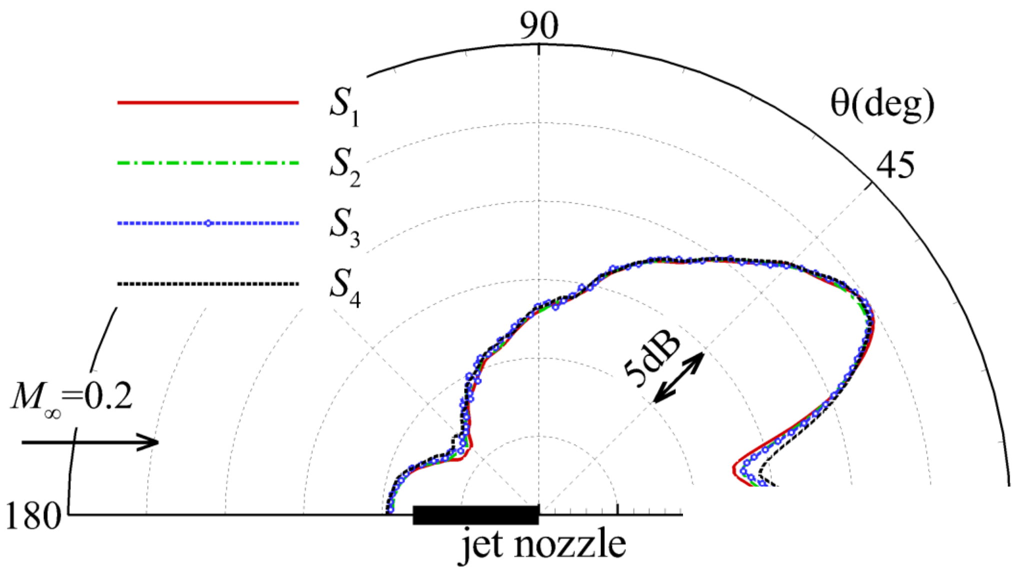

$r_o = 250D$

Results by different integration surfaces are consistent.

The prediction matches well with the DNS data measured directly.

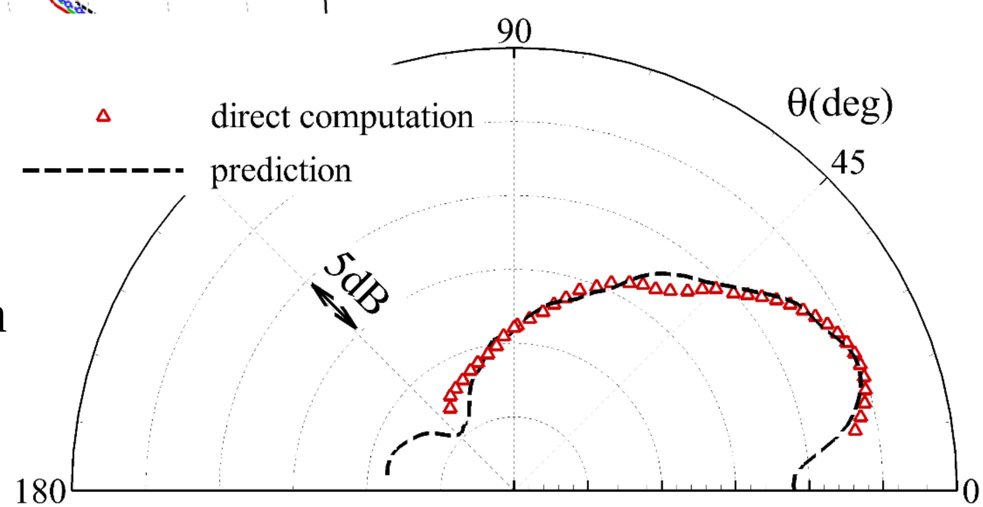

$r_o = 40D$

M1: single FW-H surface

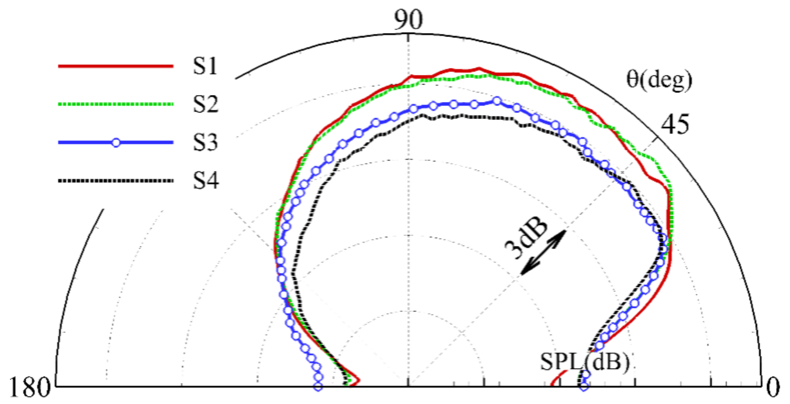

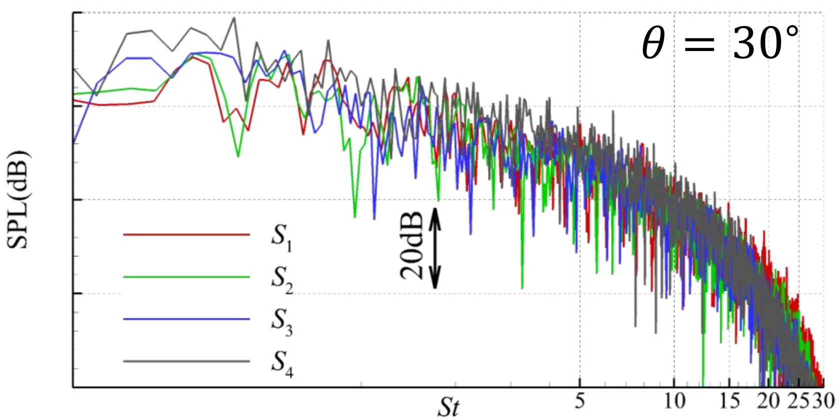

✈Results by different integration surfaces are inconsistent.

✈The far-field directivities seem to be incorrect:

- This is expected because non-acoustic components are included in the source terms .

M2: taking average of multiple FW-H surfaces

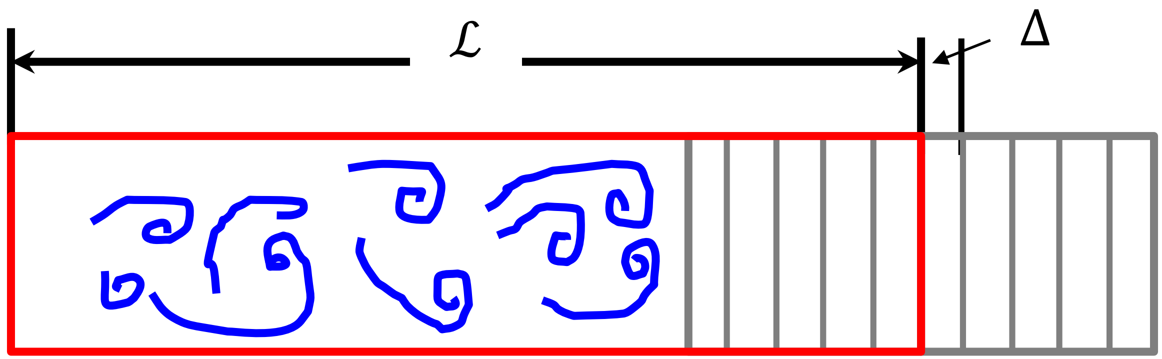

- Multiple integration surfaces are placed near the center surface.
- FW-H solution for each integration surface is computed.
- The predicted results by different integration surfaces are averaged in the frequency domain.
- The performance is influence by the number of integration surfaces, and the distance Δ
  - In this work, $\Delta = 0.5$ and the influence of N is investigated

M2: influence of the number of surfaces N

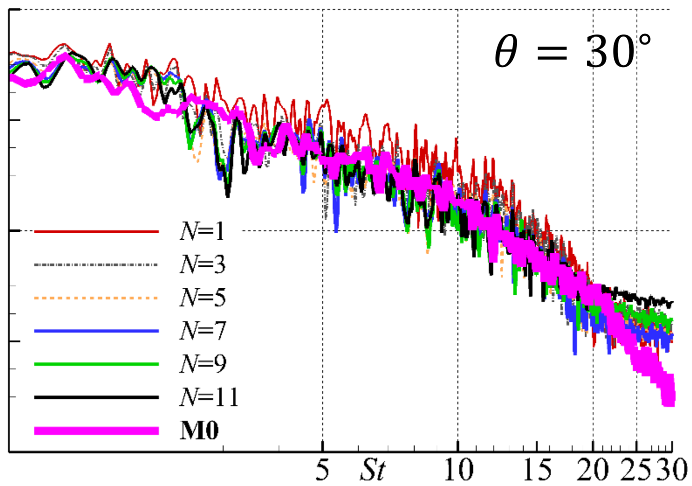

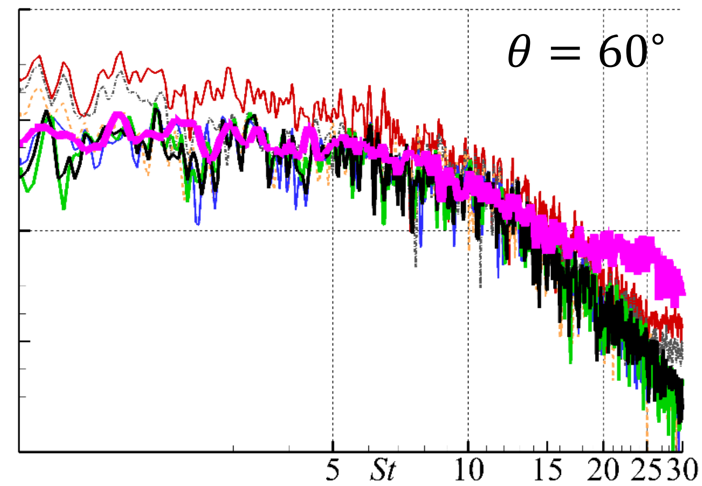

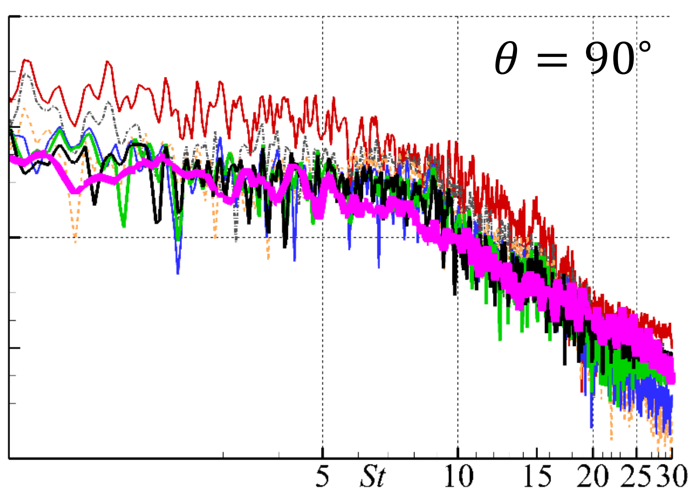

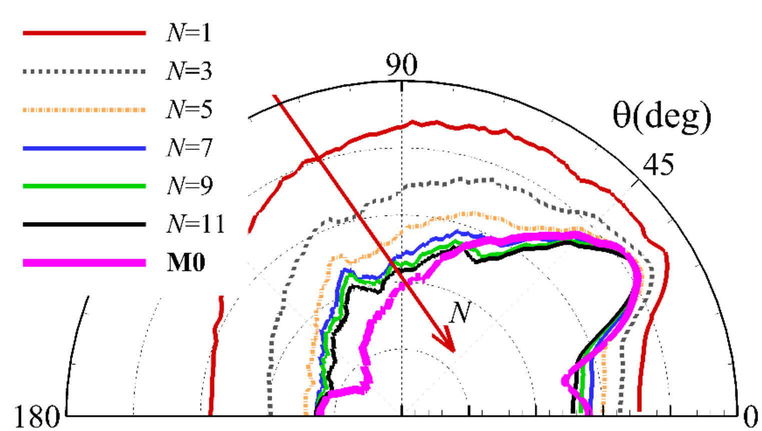

M2: influence of the centre integration surface

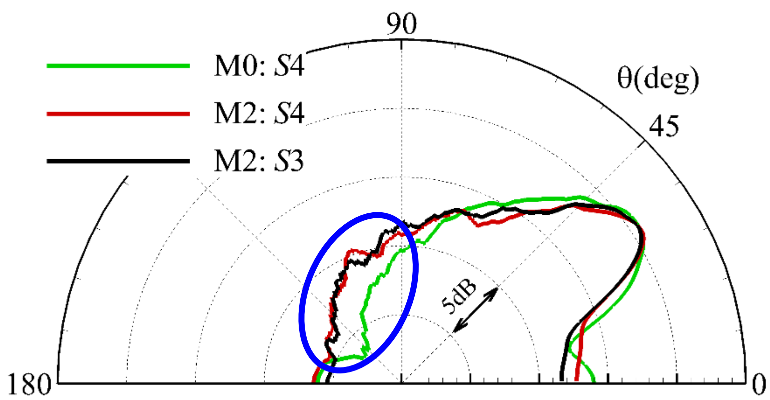

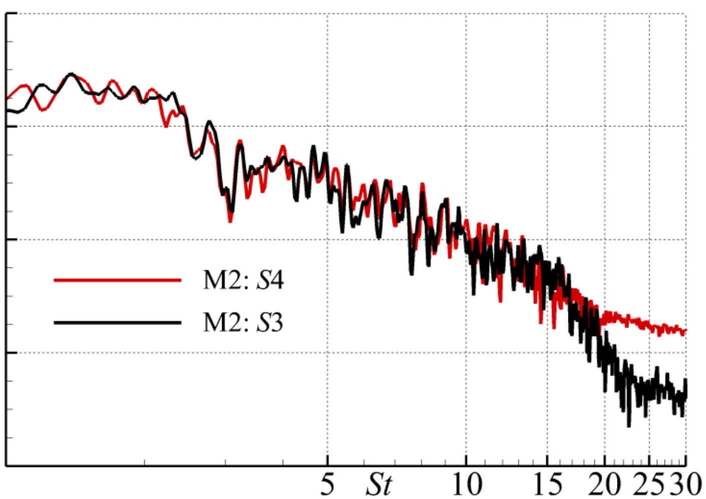

✈**M2** also gives consistent prediction results for different centre surfaces.

✈The results match reasonably well with the **M0 (**the $\mathcal{D}_c p'$ method):

- for cases with $N \geq 7$.

✈However, differences can still be found at higher observer angles:

- Results by **M2** are sensitive to N;
- More efforts are required to figure out the reason of this…

Computational cost

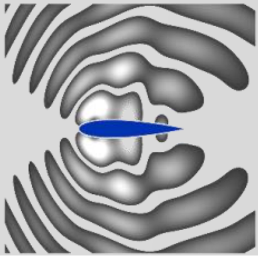

- ✈ Input variables for the FW-H solver:
  - 5 variables: ρ, $\boldsymbol{u}$, p
- ✈ Input variables for the $\mathcal{D}_c p'$ method
  - Could be only 4 variables: $q' = \mathcal{D}_c p' = \left(\frac{\partial}{\partial t} + \boldsymbol{u_0} \cdot \nabla\right) p'$, $\nabla q'$
  - For the current study using an existed CFD data, 26 variables are used to extract q' and its derivatives: ρ, $\nabla\rho$, $\boldsymbol{u}$, $\nabla\boldsymbol{u}$, p, $\nabla p'$, $\frac{\partial^2 p}{\partial x_i \partial x_j}$

Methods	M1	M2	M0
Storage (GB)	9.2	9.2×N	45.6
Time cost (s)	23299	23299×N	34466

Summary

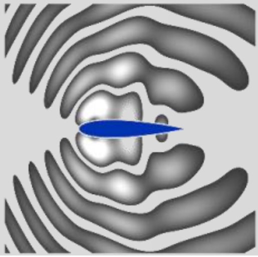

- The far-field prediction methods for turbulent flow:
  - M0: Using an indirect acoustic variable $\mathcal{D}_c p'$ to filter out the non-acoustic components.
  - M2: Taking average of multiple FW-H integration surfaces to cancel the random errors by the turbulent flow.
- Consistency: both methods can yield consistent results for different integration surfaces.
- Results by **M2** match reasonably well with **M0** at $\theta \in (0°, 75°)$ if more integration surfaces are used.
- There are difference between the results by **M0** and **M2** at high observer angles:
  - Possibly, the number and location of the integration surfaces by the **M2** method should be optimized.

Thank you for the attention!

We wish to thank Prof. Richard Sandberg from the University of Melbourne for kindly sharing the DNS database for the jet noise. Part of the work supported by the Hong Kong Innovation and Technology Commission (ref. ITS/038/15FP). The study is conducted under HK R&D ARI 1718026.

Reference

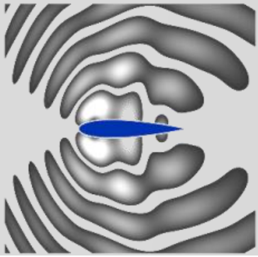

- Amiet, R. K., “Acoustic radiation from an airfoil in a turbulent stream”, *J. Sound Vib*. 41 (4), 407–420, 1975.
- Ikeda T., Enomoto S., Yamamoto K., Amemiya K., “On the modification of the Ffowcs Williams-Hawkings integration for jet noise prediction”, AIAA Paper 2013-2277, 2013.
- Kovásznay L. S. G., “Turbulence in supersonic flow”, *J. Aero. Sci.* **20**, 657–682, 1953.
- Lighthill J., “On sound generated aerodynamically. I. General theory”, *Proc. R. Soc. A*, 211, 546–587, 1952.
- Lilley G., “Appendix: Generation of sound in a mixing region”, *Fourth monthly progress report on contact F-33615-71-C-1663*. Lockheed Aircraft Co, 1971.
- Lockard D. P., “A comparison of Ffowcs Williams–Hawkings solvers for airframe noise applications”, AIAA Paper 2002-2580, 2002.
- Phillips O. M., “On the generation of sound by supersonic turbulent shear layers”, *J. Fluid Mech.* **9**, 1–28, 1960.
- Rahier G., Huet M., Peieur J., “Additional terms for the use of Ffowcs Williams and Hawkings surface integrals in turbulent flows.”, *Comput. Fluids*, 120, 158–172, 2015.

Reference

- Sandberg R. D., Tester B. J., “Mach-number scaling of individual azimuthal modes of subsonic co-flowing jets”, *J. Fluid Mech.* **793**,
- Shur M. L., Splart P. R., Strelets M. K., “Noise prediction for increasingly complex jets. Part I: methods and tests”, Intl J. Aeroacoust. 4 (3–4), 213–246, 2015.
- Splart P. R., Shur M. L., “Variants of the Ffowcs Williams–Hawkings equation and their coupling with simulations of hot jets”, Intl J. Aeroacoust. 8 (5), 477–492, 2009.
- Splart P. R., Shur M. L., Strelets M. K., Travin A. K., “Initial noise predictions for rudimentary landing gear”, J. Sound Vib. 330 (17), 4180–4195, 2011.
- Taylor G. I., “The spectrum of turbulence”, *Proc. R. Soc. A* **164**, 476–490, 1938209–228, 2016.
- Wright M. C., Morfey C. L., “On the extrapolation of acoustic waves from flow simulations with vortical out flow”, Int. J. Aeroacoust., 14 (1–2), 217–227, 2015.
- Zhong S. Y., Zhang X., “A sound extrapolation method for aeroacoustics far-field prediction in presence of vortical waves”, J. Fluid Mech., 820, 424-450, 2017
- Zhong S. Y., Zhang X., “A generalized sound extrapolation method for turbulent flows”, *Proc. R. Soc. A.*, 474, 2017614, 2018.

Cylinder flow noise

- $M_\infty = 0.2$, and $R_e = 1000$.
- The loading noise is the dominant source of sound:
  - The on-body FW-H method can yield an accurate prediction.

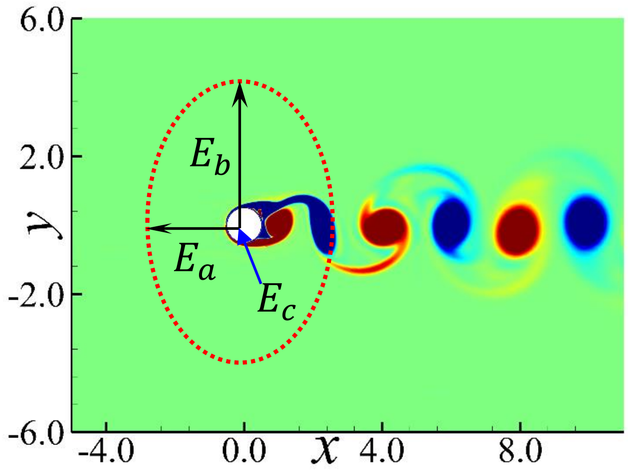

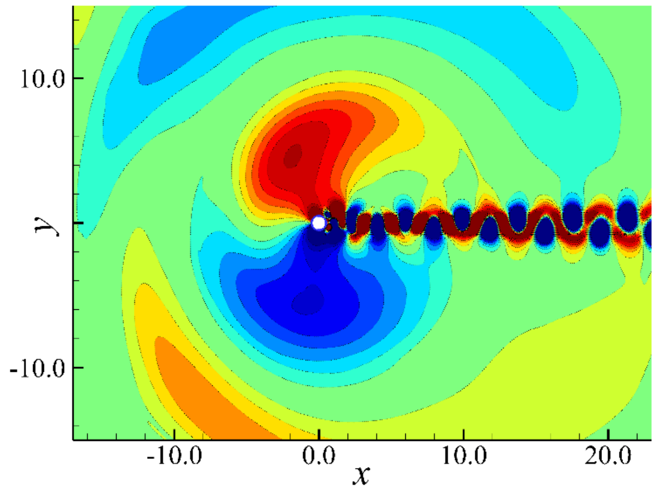

	S1	S2	S3	S4	S5	S6	S7
E_a	2	3	4	5	5	5	5
E_b	2	3	4	4	4	4	5
E_c	0	0	0	0	1	2	3

Spectra at $\theta = 90°$ by the $\mathcal{D}_c p'$ method

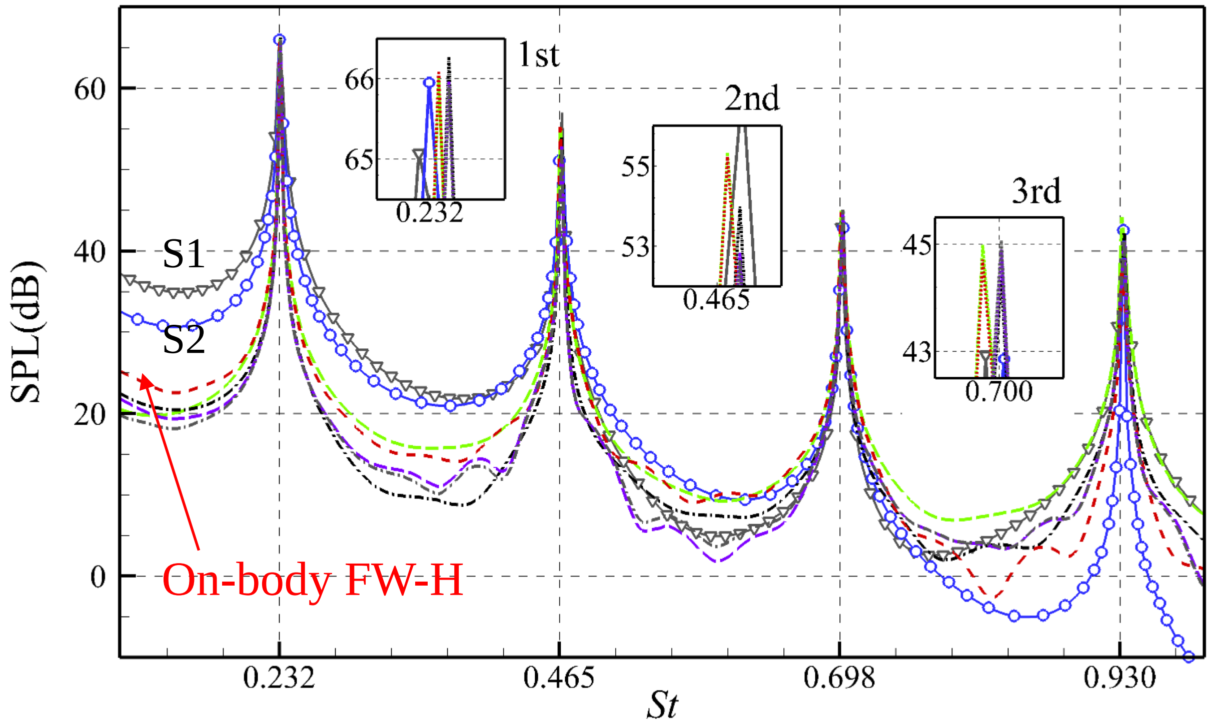

✈ Larger errors by S1 and S2 where the vortices are still developing.

✈ Results by other surfaces are close to the on-body FW-H method.

Predictions by the $\mathcal{D}_c p'$ method

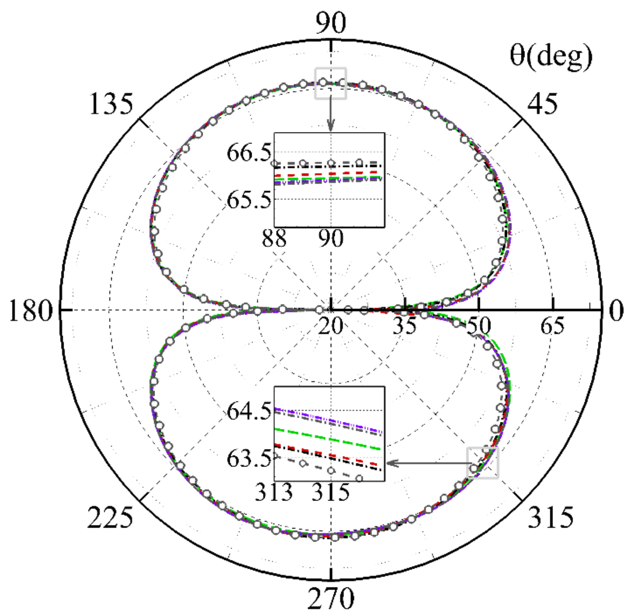

1st harmonic

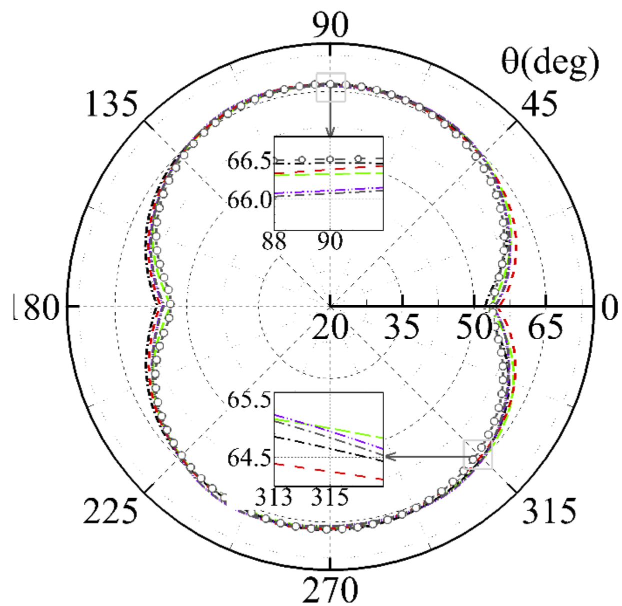

OASPL

- Relatively larger errors at low/high observer angles.
- The off-body predictions match fairly well with the on-body FW-H results.

M3: filter out the vortical wave

- For turbulent flows, non-acoustic components are contained in the surface source terms of the FW-H equation

- A rearrangement of the FW-H equation (Zhong & Zhang, 2017)

$$\left(\frac{\partial}{\partial t}+\boldsymbol{u}_\infty\cdot\nabla\right)^2 p'-c_\infty^2\nabla^2 p'=\frac{DS_p}{Dt}-\gamma p_0\nabla\cdot\boldsymbol{S}_u.$$

- The formulation of the source terms S_p and $\boldsymbol{S_u}$

$$\boldsymbol{S}_u=\left[(\boldsymbol{u}_\infty-\boldsymbol{u_0})\cdot\nabla\boldsymbol{u}'+\left(\frac{1}{\rho_\infty}-\frac{1}{\rho_0}\right)\nabla p'\right]-\left[\boldsymbol{u}'\cdot\nabla\boldsymbol{u_0}-\frac{\rho'\nabla p_0}{\rho_0(\rho_0+\rho')}\right]-\left[\boldsymbol{u}'\cdot\nabla\boldsymbol{u}'-\frac{\rho'\nabla p'}{\rho_0(\rho_0+\rho')}\right]$$

$$S_p=[(\boldsymbol{u}_\infty-\boldsymbol{u_0})\cdot\nabla p'+\gamma(p_\infty-p_0)\nabla\cdot\boldsymbol{u}']-[\boldsymbol{u}'\cdot\nabla p_0+\gamma p'\nabla\cdot\boldsymbol{u_0}]-[\boldsymbol{u}'\cdot\nabla p'+\gamma p'\nabla\cdot\boldsymbol{u}']$$

- The $\nabla\cdot$ and $D=\dfrac{\partial}{\partial t}+\boldsymbol{u}_\infty\cdot\nabla$ are act on $\boldsymbol{u}'$
  - Non-acoustic components are efficiently filtered out for turbulences dominated by vortical waves

M3: filter out the vortical wave

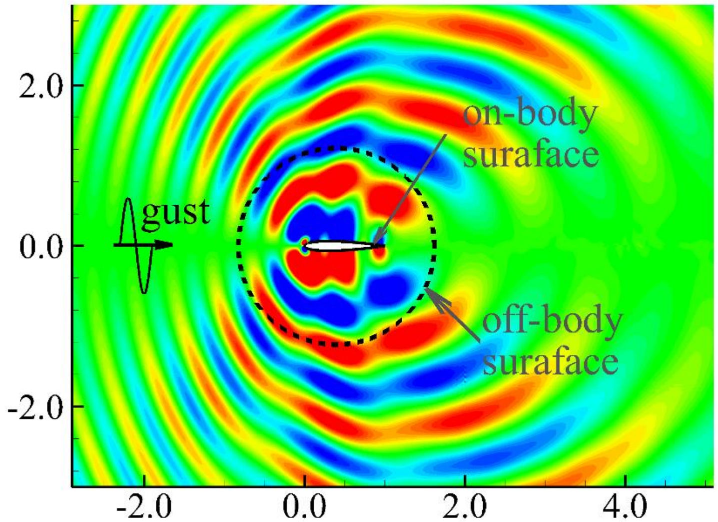

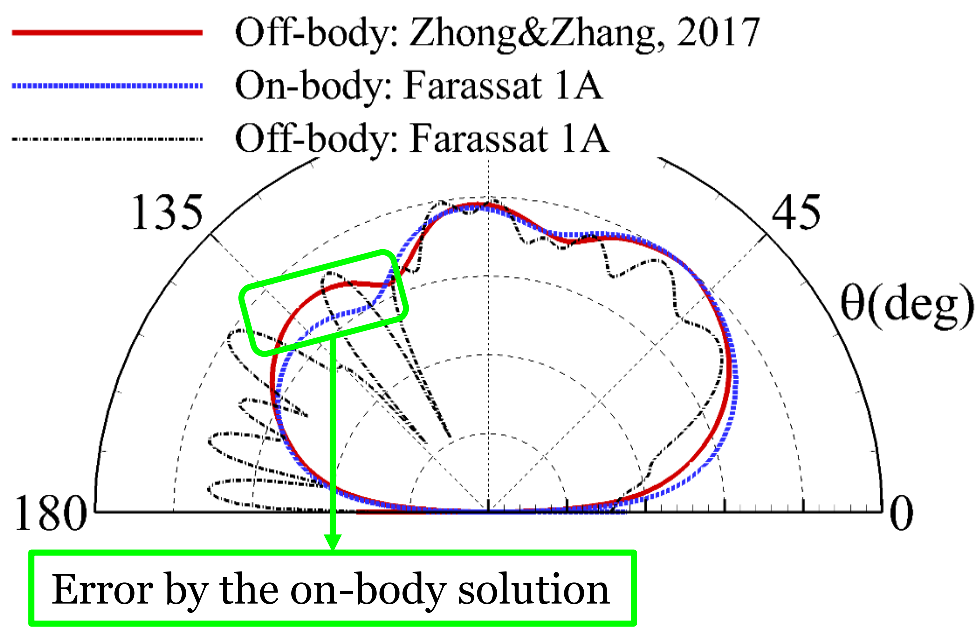

- The vortical waves can be filtered out based on the divergence-free and convection motion properties (Zhong & Zhang, 2017).
- However, convecting (non-acoustic) pressure fluctuations are also included in the surface sources (for general turbulent flows).

Results by filtering vortical waves

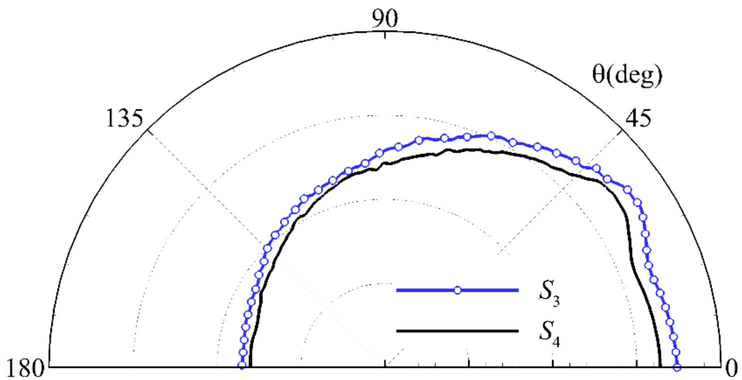

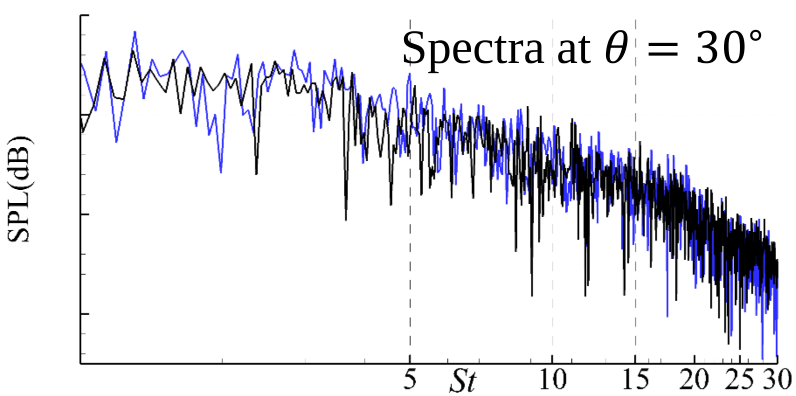

- Results by different integration surfaces are inconsistent
- The predicted far-field directivities seem to be incorrect
- The turbulence contains not only vortical waves, but also convecting pressure fluctuations
- The turbulent velocity components is also not divergence free in the jet region

“Sources” of different acoustic analogies